# Supporting Information

# Peroxidase vs. Peroxygenase Activity: Substrate Substituent Effects as Modulators of Enzyme Function in the Multifunctional Catalytic Globin Dehaloperoxidase

Ashlyn H. McGuire, Leiah M. Carey, Vesna de Serrano, Safaa Dali, and Reza A. Ghiladi*
Department of Chemistry, North Carolina State University, Raleigh, North Carolina, 27695

**Table of Contents**

**Figure S8.** Kinetic data for the reaction of $H_2O_2$-activated DHP B with 4-Me-G, 5-Br-G, and 6-Br-G.

**Figure S9.** Stopped-flow spectroscopic monitoring of the reaction of ferric DHP B with 2-MeOBQ.

**Figure S10.** *Top*: plot of $k_{obs}$ vs [2-MeOBQ] using the data obtained from Figure S9 for the reduction of WT ferric DHP B by 2-MeOBQ (0.625-625 μM) yielding the oxyferrous-like DHP species; inset: corresponding double-reciprocal plot ($1/k_{obs}$ vs 1/[2-MeOBQ]). *Bottom*: rate constants determined from the SVD analysis of the data presented in Figure S9.

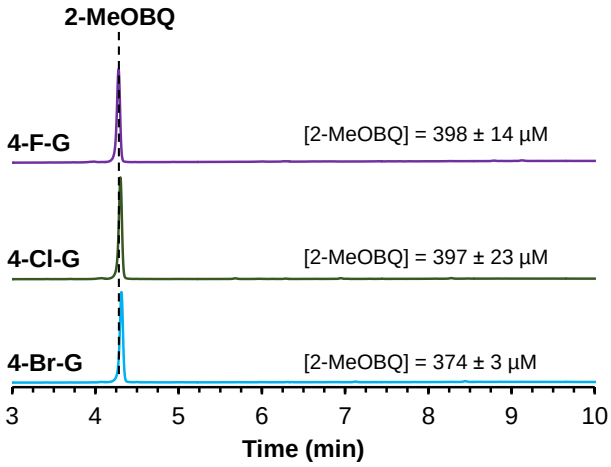


**Figure S1.** HPLC chromatograms (260 nm) of the reaction of 500 µM 4-X-guaiacol with 10 µM DHP B in the presence of 500 µM $H_2O_2$ at 25 °C in 5 % MeOH/100 mM $KP_i$ (v/v) at pH 7. The reaction was quenched after 5 minutes with the addition of excess catalase. The 2-MeOBQ product is highlighted at $t_R = 4.3$ min.

**Table S1.** Guaiacol reaction products detected using LC-MS (positive ion mode).

| Substrate | Product $t_R$ (min) | *m/z* | Molecular Formula | Description | Footnotes |
|---|---|---|---|---|---|
| ***o*-guaiacol** | 3.9 | 139.04 | $C_7H_6O_3$ | Monomer, +1 O - 2 H; 2-MeOBQ | *a* |
| | 6.4 | 245.08 | $C_{14}H_{12}O_4$ | Dimer, - 2 H | |
| | 8.0 | 367.12 | $C_{21}H_{18}O_6$ | Trimer, - 2 H | |
| | 11.5 | 489.15 | $C_{28}H_{24}O_8$ | Tetramer, – 2 H | |
| **4-Br-guaiacol** | 3.9 | 139.04 | $C_7H_6O_3$ | Monomer +1 O - 2 H; 2-MeOBQ | *a, b* |
| | 7.1 | 277.07 | $C_{14}H_{12}O_6$ | Dimer +2 OH -2 Br, 2 H | |
| | 8.5 | 261.08 | $C_{14}H_{12}O_5$ | Dimer +1 OH -2 Br, 2 H | |
| | 9.7 | 308.98 | $C_{13}H_9O_4Br$ | Dimer - 1 $CH_3$, 1 Br, 1 H | |
| | 12.0 | 461.02 | $C_{21}H_{17}O_7Br$ | Trimer + 1 OH - 2 Br, 1 H | |
| | 12.1 | 431.01 | $C_{20}H_{15}O_6Br$ | Trimer + 1 H - 1 $CH_3$, 2 Br | |
| **4-Cl-guaiacol** | 3.9 | 139.04 | $C_7H_6O_3$ | Monomer +1 O - 2 H; 2-MeOBQ | *a, b* |
| | 7.1 | 277.07 | $C_{14}H_{12}O_6$ | Dimer +2 OH -2 Cl, 2 H | |
| | 8.4 | 261.08 | $C_{14}H_{12}O_5$ | Dimer +1 OH -2 Cl, 2 H | |
| | 9.4 | 265.03 | $C_{13}H_9O_4Cl$ | Dimer - 1 $CH_3$, 1 Cl, 1 H | |
| | 11.8 | 417.07 | $C_{21}H_{17}O_7Cl$ | Dimer + 1 O, 2 Cl | |
| | 11.9 | 387.06 | $C_{20}H_{15}O_6Cl$ | Trimer - 1 $CH_3$, 2 Cl, | |
| | 13.3 | 509.10 | $C_{27}H_{21}O_8Cl$ | Tetramer + 2 H - 1 $CH_3$, 3 Cl | |
| **4-F-guaiacol** | 3.9 | 139.04 | $C_7H_6O_3$ | Monomer +1 O - 2 H; 2-MeOBQ | *a, b* |
| | 7.1 | 277.07 | $C_{14}H_{12}O_6$ | Dimer +2 OH -2 F, 2 H | |
| | 7.1 | 575.12 | $C_{28}H_{21}O_9F_3$ | Tetramer + 1 O - 1 F, 1 H | |
| | 8.4 | 261.08 | $C_{14}H_{12}O_5$ | Dimer +1 OH -2 Br, 2 H | |
| | 10.9 | 383.11 | $C_{21}H_{18}O_7$ | Trimer + 1 OH - 3 F | |

[a] Compared to an authentic (commercial) sample of 2-MeOBQ.
[b] Only product observed when monitored via HPLC (UV/vis spectroscopic detection).

**Table S2.** Guaiacol reaction products detected using LC-MS (negative ion mode).

| Substrate | Product $t_R$ (min) | *m/z* | Molecular Formula | Description | Footnotes |
|---|---|---|---|---|---|
| **5-Br-guaiacol** | 9.5 | 400.09 | $C_{14}H_{12}O_4Br_2$ | Dimer | |
| | 11.6 | 600.85 | $C_{21}H_{17}O_6Br_3$ | Trimer | |
| | 12.2 | 520.92 | $C_{21}H_{16}O_6Br_2$ | Trimer - 1 Br, 1 H | |
| | 13.8 | 720.87 | $C_{28}H_{21}O_8Br_3$ | Tetramer - 1 Br, 1 H | |
| | 13.0 | 800.8 | $C_{28}H_{22}O_8Br_4$ | Tetramer | |
| **6-Br-guaiacol** | 8.4 | 336.97 | $C_{14}H_{11}O_5Br$ | Dimer + 1 OH - 1 Br | |
| | 10.1 | 658.96 | $C_{28}H_{22}O_9Br_2$ | Tetramer + 1 OH - 2 Br, 1 H | |
| | 10.4 | 400.9 | $C_{14}H_{12}O_4Br_2$ | Dimer | |
| | 11.5 | 736.87 | $C_{28}H_{21}O_9Br_3$ | Tetramer + 1 OH - 1 Br | |
| | 11.7 | 506.91 | $C_{20}H_{14}O_6Br_2$ | Trimer - 1 $CH_3$, 1 Br | |
| | 11.7 | 706.86 | $C_{27}H_{18}O_8Br_3$ | Tetramer - 1 $CH_3$, 1 Br | |
| | 12.7 | 600.85 | $C_{21}H_{17}O_6Br_3$ | Trimer | |
| | 12.9 | 722.89 | $C_{28}H_{23}O_8Br_4$ | Tetramer + 1 H - 1 Br | |
| | 14.4 | 800.8 | $C_{28}H_{22}O_8Br_4$ | Tetramer | |
| **4-$NO_2$-guaiacol** | 3.8 | 139.04 | $C_7H_6O_3$ | Monomer +1 O - 2 H; 2-MeOBQ | *a* |
| | 6.5 | 168.03 | $C_7H_7NO_4$ | Monomer | |
| | 8.1 | 304.05 | $C_{14}H_{11}NO_7$ | Dimer + 1 O - 1 $NO_2$, 1 H | |
| | 8.6 | 276.05 | $C_{13}H_{11}NO_6$ | Dimer + 1 OH, 1 H - 1 $NO_2$, 1 $OCH_3$ | |
| | 9.6 | 335.05 | $C_{14}H_{12}N_2O_8$ | Dimer | |
| | 10.5 | 443.07 | $C_{20}H_{16}N_2O_{10}$ | Trimer + 2 H - 1 $NO_2$, 1 $CH_3$ | |
| | 10.7 | 441.06 | $C_{20}H_{14}N_2O_{10}$ | Trimer - 1 $NO_2$, 1 $CH_3$ | |
| | 11.2 | 457.09 | $C_{21}H_{18}N_2O_{10}$ | Trimer - 1 $NO_2$ | |
| | 11.6 | 518.07 | $C_{21}H_{17}N_3O_{13}$ | Trimer + 1 O | |
| | 11.8 | 288.02 | $C_{13}H_7NO_7$ | Dimer + 1 O - 1 $NO_2$ - 1 $CH_3$ - 2 H | |
| **4-MeO-guaiacol** | 3.7 | 323.04 | $C_{14}H_{12}O_9$ | Dimer +3 OH - 2 $CH_3$, 3 H | |
| | 3.8 | 139.04 | $C_7H_6O_3$ | Monomer +1 O - 2 H; 2-MeOBQ | *a* |
| | 4.4 | 289.04 | $C_{14}H_{10}O_7$ | Dimer + 1 OH -2 $CH_3$, 2 H | |
| | 6.2 | 425.05 | $C_{21}H_{14}O_{10}$ | Trimer + 1 OH - 3 $CH_3$, 2 H | |
| | 6.4 | 275.05 | $C_{14}H_{12}O_6$ | Dimer - 2 $CH_3$ | |
| | 6.0 | 445.11 | $C_{22}H_{22}O_{10}$ | Trimer + 1 OH, 2 H - 2 $CH_3$, 1 H | |
| | 6.7 | 427.10 | $C_{22}H_{20}O_9$ | Trimer - 2 $CH_3$ | |
| | 6.2 | 443.13 | $C_{23}H_{24}O_9$ | Trimer + 1 H - 1 $CH_3$ | |
| | 8.5 | 425.09 | $C_{22}H_{16}O_9$ | Trimer - 2 $CH_3$, 4 H | |
| | 8.6 | 305.1 | $C_{16}H_{18}O_6$ | Dimer | |
| | 9.1 | 579.15 | $C_{30}H_{28}O_{12}$ | Tetramer - 2 $CH_3$ | |

[a] Detected in positive ion mode.

**Table S2 (continued).**

| Substrate | Product $t_R$ (min) | *m/z* | Molecular Formula | Description | Footnotes |
|---|---|---|---|---|---|
| **4-Me-guaiacol** | 5.2 | 305.1 | $C_{16}H_{18}O_6$ | Dimer + 2 OH - 2 H | |
| | 6.2 | 303.09 | $C_{16}H_{16}O_6$ | Dimer + 2 OH - 4 H | |
| | 7.5 | 289.11 | $C_{16}H_{18}O_5$ | Dimer + 1 OH - 1 H | |
| | 7.8 | 273.08 | $C_{15}H_{14}O_5$ | Dimer + 1 OH - 1 $CH_3$, 2 H | |
| | 10.0 | 439.14 | $C_{24}H_{24}O_8$ | Trimer + 2 OH - 4 H | |
| | 13.0 | 273.11 | $C_{16}H_{18}O_4$ | Dimer | |
| | 13.9 | 409.16 | $C_{24}H_{25}O_6$ | Trimer | |

[a] Detected in positive ion mode.

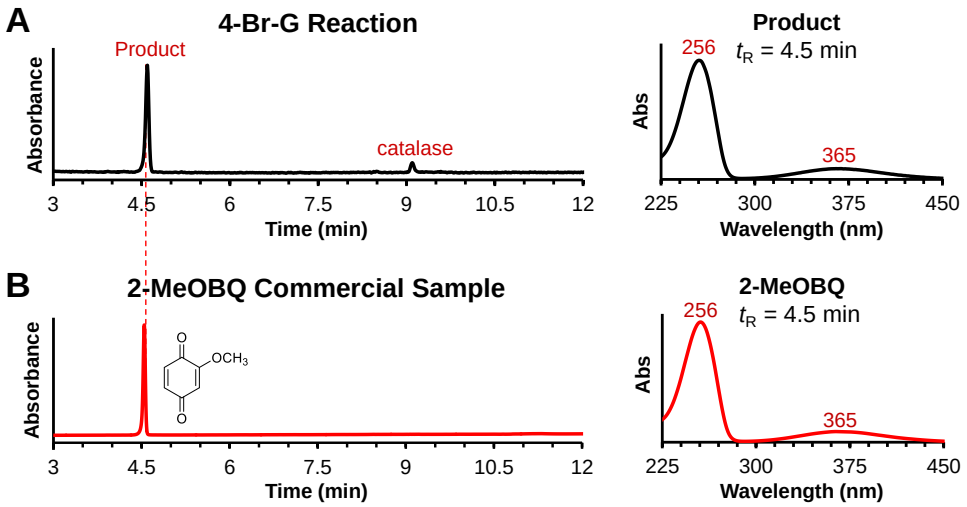


**Figure S2.** A) HPLC chromatogram (260 nm) of the reaction of 500 µM 4-Br-guaiacol with 10 µM DHP B in the presence of 500 µM $H_2O_2$ at 25 °C in 5 % MeOH/100 mM $KP_i$ (v/v) at pH 7, and the corresponding UV-visible spectrum of the reaction product ($t_R$ = 4.5 min). The reaction was quenched after 5 minutes with the addition of excess catalase ($t_R$ = 9 min). B) An authentic sample of 2-MeOBQ under identical elution conditions as panel A, and its corresponding UV-visible spectrum.

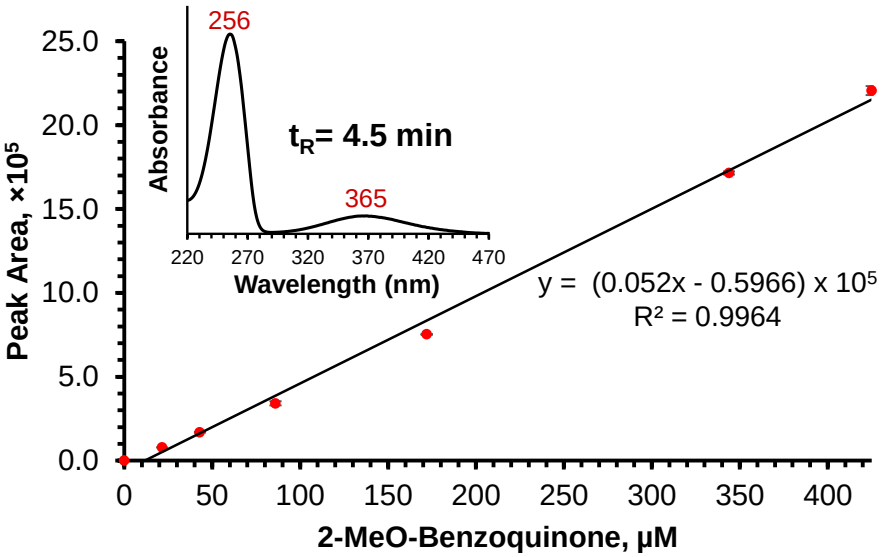


**Figure S3.** HPLC calibration curve for quantification of 2-MeOBQ (0 – 425 µM); inset: UV-visible spectrum of 2-MeOBQ obtained from the HPLC chromatogram ($t_R$ = 4.5 min).

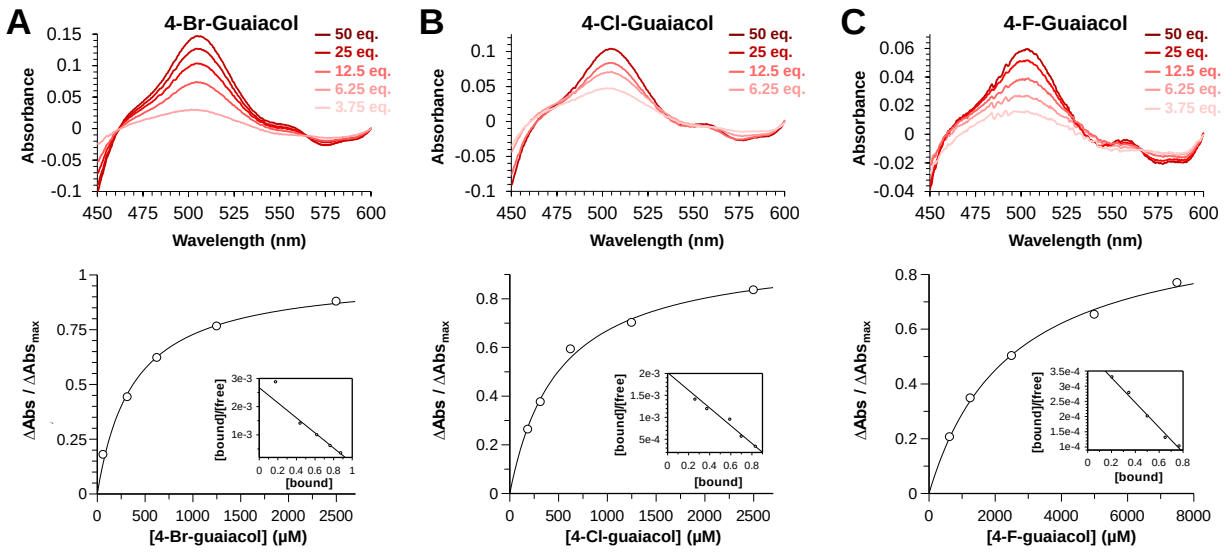


**Figure S4.** Optical difference spectra (top) and titration curves (bottom) of 4-X-guaiacol binding (3.75-50 eq) to 25 μM DHP B in 5 % MeOH / 100 mM $KP_i$ (v/v) at pH 7 for A) 4-Br-guaiacol, B) 4-Cl-guaiacol, and C) 4-F-guaiacol. *Insets*: corresponding Scatchard plots (ratio of concentrations of bound ligand to unbound ligand versus the bound ligand concentration).

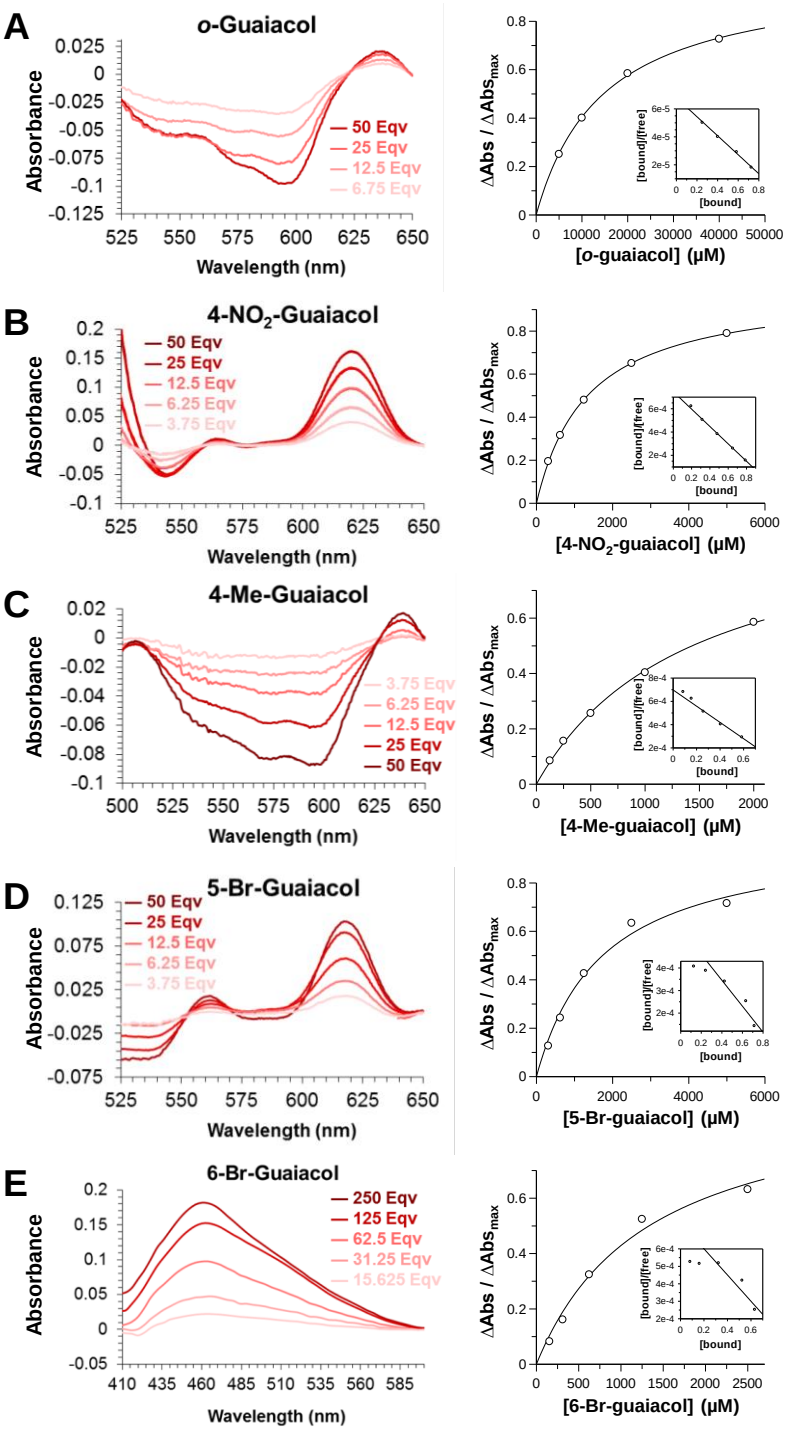


**Figure S5.** Optical difference spectra (left) and titration curves (right) of guaiacol binding (3.75-250 eq) to 25 μM DHP B in 5 % MeOH / 100 mM KPi (v/v) at pH 7 for A) *o*-guaiacol, B) 4-$NO_2$-guaiacol, C) 4-Me-guaiacol, D) 5-Br-guaiacol, and E) 6-Br-guaiacol. *Insets*: corresponding Scatchard plots (ratio of concentrations of bound ligand to unbound ligand versus the bound ligand concentration).

**Table S3.** X-ray data collection and refinement statistics for DHP B in complex with 4-bromo-*o*-guaiacol, (6CKE), 5-bromo-*o*-guaiacol, (6CRE), 6-bromo-*o*-guaiacol, (6CO5), 4-nitro-*o*-guaiacol (6CH5) and 4-methoxy-*o*-guaiacol (6CH6).

| | **4-Br-G** | **5-Br-G** | **6-Br-G** | **4-$NO_2$-G** | **4-MeO-G** |
|---|---|---|---|---|---|
| PDB Entry | 6CKE | 6CRE | 6CO5 | 6CH5 | 6CH6 |
| Data Collection | | | | | |
| Wavelength (Å) | 1.00 | 1.00 | 1.00 | 1.00 | 1.00 |
| Temperature (K) | 100 | 100 | 100 | 100 | 100 |
| Space Group | $P2_12_12_1$ | $P2_12_12_1$ | $P2_12_12_1$ | $P2_12_12_1$ | $P2_12_12_1$ |
| Unit-cell parameters (Å) | | | | | |
| *a* | 59.40 | 59.22 | 59.52 | 59.65 | 59.79 |
| *b* | 66.45 | 66.19 | 66.14 | 66.37 | 66.35 |
| *c* | 68.21 | 68.20 | 68.39 | 68.22 | 68.29 |
| Unique reflections | 57,274 (2,821)[a] | 36,635 (1,809) | 30,799 (1,511) | 31,440 (2,214) | 29,059 (2,117) |
| Completeness (%) | 99.9 (100) | 97.8 (99.1) | 99.4 (99.0) | 99.3 (96.8) | 99.97 (99.86) |
| $R_{merge}$ (%)[b] | 7.5 (66.2) | 12.9 (86.3) | 11.9 (79.6) | 7.6 (37.3) | 11.1 (64.0) |
| $R_{pim}$ (%)[c] | 3.7 (33.9) | 6.2 (42.9) | 6.0 (41.6) | 4.1 (17.9) | 5.6 (32.5) |
| $CC_{1/2}$[d] | 0.746 | 0.642 | 0.553 | 0.906 | 0.776 |
| $I/\sigma_{(I)}$ | 22.4 (1.9) | 13.7 (2.0) | 14.1 (1.9) | 19.8 (3.3) | 16.9 (2.7) |
| Redundancy | 4.8 (4.7) | 4.9 (4.8) | 4.8 (4.7) | 4.3 (3.9) | 4.8 (4.8) |
| Refinement | | | | | |
| Resolution (Å) | 1.37 | 1.58 | 1.69 | 1.65 | 1.70 |
| $R_{work}$ (%)[e] | 17.42 (25.19) | 16.34 (21.99) | 16.68 (19.95) | 15.26 (24.1) | 16.2 (34.1) |
| $R_{free}$ (%)[f] | 19.27 (27.84) | 21.17 (25.77) | 20.89 (24.91) | 20.56 (28.7) | 22.73 (41.4) |
| No. of protein atoms | 2,470 | 2,294 | 2,339 | 2,721 | 2,676 |
| No. of solvent atoms | 413 | 392 | 406 | 260 | 289 |
| R.m.s.d from ideal geometry[g] | | | | | |
| Bond lengths (Å) | 0.007 | 0.007 | 0.007 | 0.013 | 0.015 |
| Bond angles (°) | 0.916 | 0.910 | 0.922 | 1.697 | 1.71 |
| Ramachandran plot (%)[h] | | | | | |
| Most favored region | 98.49 | 97.78 | 98.50 | 99.1 | 98.5 |
| Addl allowed region | 1.13 | 2.22 | 1.50 | 0.9 | 1.5 |
| Outliers | 0.38 | ---- | ---- | 0 | 0 |

[a]Values in parentheses are for the highest resolution shell. [b]$R_{merge} = \sum_{hkl}\sum_i[|I_i(hkl) - \langle I(hkl)\rangle| / \sum_{hkl}\sum_i I(hkl)] \times 100$, where $I_i(hkl)$ is the $i^{th}$ measurement and $\langle I(hkl)\rangle$ is the weighted mean of all measurements of I(hkl). [c]$R_{pim} = \sum_{hkl}\sqrt{1/n-1}\sum_i[|I_i(hkl) - \langle I(hkl)\rangle| / \sum_h\sum_i I(hkl)] \times 100$. [d]$CC_{1/2} = \sum(x - \langle x\rangle)(y - \langle y\rangle) / [\sum(x - \langle x\rangle)^2 \sum(y - \langle y\rangle)^2]^{1/2}$. [e]$R_{work} = \sum|F_O - F_C|/\sum F_O \times 100\%$, where $F_O$ and $F_C$ are the observed and calculated structure factors, respectively. [f]$R_{free}$ is the R factor for the subset (5-10 %) of reflections selected before and not included in the refinement. [g]Root-mean-square deviation. [h]Ramachandran plot created via MolProbity.

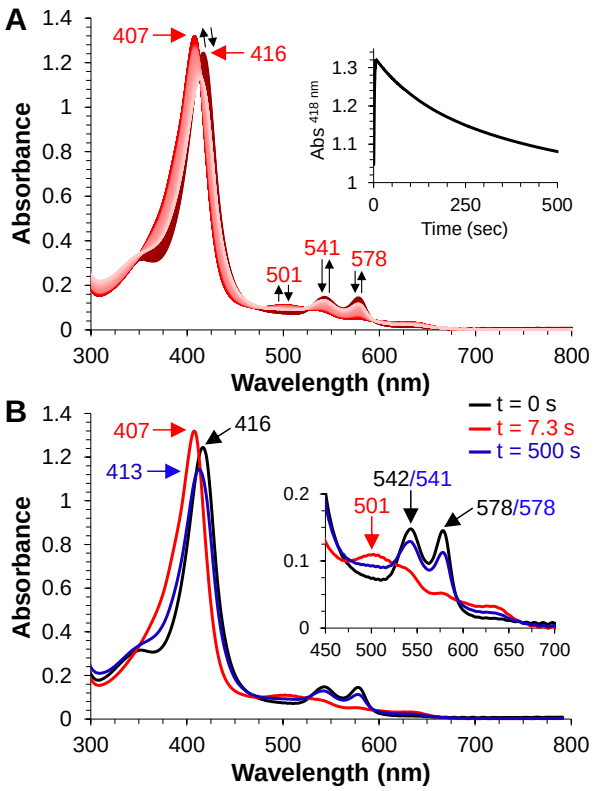


**Figure S6.** Kinetic data for the reaction of oxyferrous DHP B with 4-Br-guaiacol. A) Stopped-flow UV−visible spectra of the double-mixing reaction between oxyferrous DHP B (10 μM) premixed with 10 eq. of $H_2O_2$ (500 ms) and then reacted with 10 eq. 4-Br-guaiacol at pH 7.0 (900 scans over 500 s); inset: the single wavelength (418 nm) dependence on time obtained from the raw data. B) Experimentally obtained spectra of oxyferrous DHP B (black, t = 0 s) reacted with 4-Br-guaiacol, resulting in ferric DHP B (red, t = 7.3 s) and further reduction to oxyferrous DHP B (blue, t = 500 s).

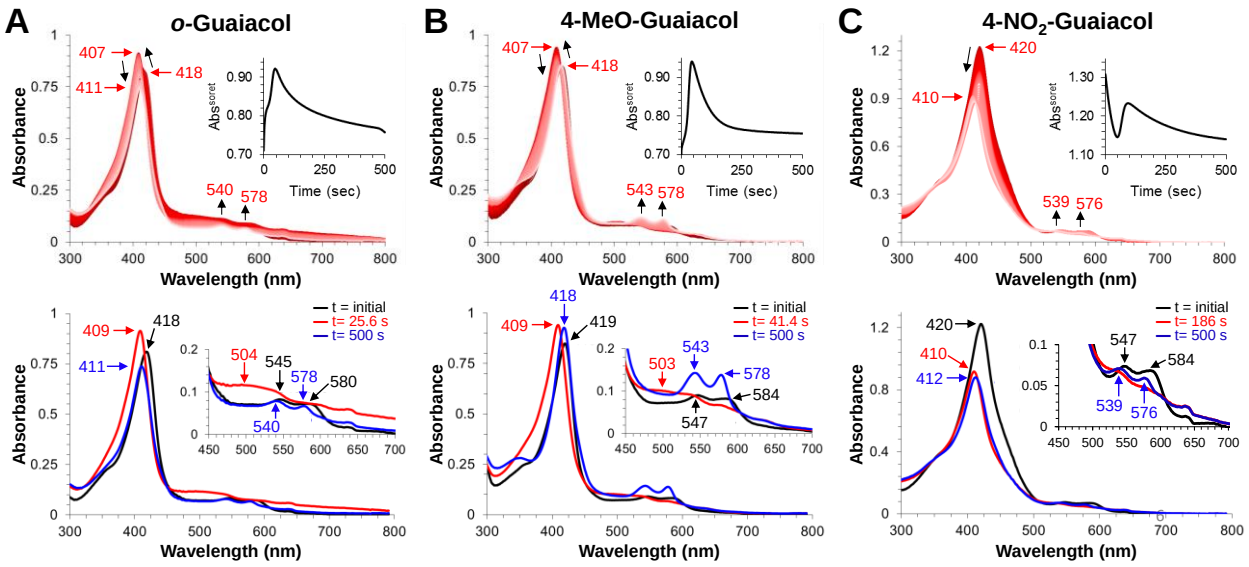


**Figure S7.** Kinetic data for the reaction of preformed DHP B Compound ES with o-G, 4-MeO-G and 4-$NO_2$-G. **A) *o*-Guaiacol:** *top panel*, stopped-flow UV−visible spectra of the double-mixing reaction between ferric DHP B (10 μM) premixed with 10 eq. of $H_2O_2$ (500 ms) and then reacted with 10 eq. *o*-guaiacol at pH 7.0 (900 scans over 500 s); inset: the single wavelength (408 nm) dependence on time obtained from the raw data; *bottom panel*, experimentally obtained spectra of Compound ES (black, t = 0 s) reacted with *o*-guaiacol, resulting in ferric DHP B (red, t = 25.6 s) and further reduction to oxyferrous DHP B (blue, t = 500 s). **B) 4-MeO-guaiacol:** *top panel*, stopped-flow UV−visible spectra of the double-mixing reaction between ferric DHP B (10 μM) premixed with 10 eq. of $H_2O_2$ (500 ms) and then reacted with 10 eq. 4-MeO-guaiacol at pH 7.0 (900 scans over 500 s); inset: the single wavelength (408 nm) dependence on time obtained from the raw data; *bottom panel*, experimentally obtained spectra of Compound ES (black, t = 0 s) reacted with 4-MeO-guaiacol, resulting in ferric DHP B (red, t = 41.4 s) and further reduction to oxyferrous DHP B (blue, t = 500 s). **C) 4-$NO_2$-guaiacol:** *top panel*, stopped-flow UV−visible spectra of the double-mixing reaction between ferric DHP B (10 μM) premixed with 10 eq. of $H_2O_2$ (500 ms) and then reacted with 10 eq. 4-$NO_2$-guaiacol at pH 7.0 (900 scans over 500 s); inset: the single wavelength (408 nm) dependence on time obtained from the raw data; *bottom panel*, experimentally obtained spectra of Compound ES (black, t = 0 s) reacted with 4-MeO-guaiacol, resulting in ferric DHP B (red, t = 186 s) and further reduction to oxyferrous DHP B (blue, t = 500 s).

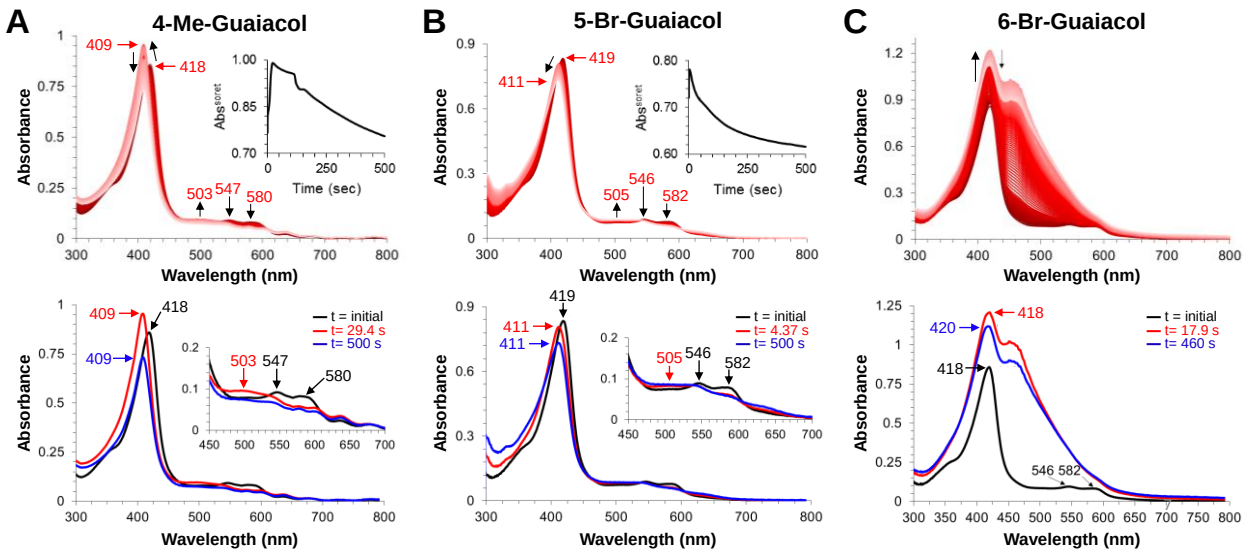


**Figure S8.** Kinetic data for the reaction of preformed DHP B Compound ES with 4-Me-G, 5-Br-G, and 6-Br-G. **A) 4-Me-guaiacol:** *top panel*, stopped-flow UV−visible spectra of the double-mixing reaction between ferric DHP B (10 μM) premixed with 10 eq. of $H_2O_2$ (500 ms) and then reacted with 10 eq. 4-Me-guaiacol at pH 7.0 (900 scans over 500 s); inset: the single wavelength (408 nm) dependence on time obtained from the raw data; *bottom panel*, experimentally obtained spectra of Compound ES (black, t = 0 s) reacted with 4-Me-guaiacol, resulting in ferric DHP B (red, t = 29.4 s) that was slowly reduced and approached a Compound RH-like species (blue, t = 500 s). **B) 5-Br-guaiacol:** *top panel*, stopped-flow UV−visible spectra of the double-mixing reaction between ferric DHP B (10 μM) premixed with 10 eq. of $H_2O_2$ (500 ms) and then reacted with 10 eq. 5-Br-guaiacol at pH 7.0 (900 scans over 500 s); inset: the single wavelength (408 nm) dependence on time obtained from the raw data; *bottom panel*, experimentally obtained spectra of Compound ES (black, t = 0 s) reacted with 5-Br-guaiacol, resulting in ferric DHP B (red, t = 4.37 s) and further reduction to a Ferric/Compound RH mixture (blue, t = 500 s). **C) 6-Br-guaiacol:** *top panel*, stopped-flow UV−visible spectra of the double-mixing reaction between ferric DHP B (10 μM) premixed with 10 eq. of $H_2O_2$ (500 ms) and then reacted with 5 eq. 6-Br-guaiacol at pH 7.0 (900 scans over 500 s); inset: the single wavelength (408 nm) dependence on time obtained from the raw data; *bottom panel*, experimentally obtained spectra of Compound ES (black, t = 0 s) reacted with 6-Br-guaiacol, resulting in an increase of absorbance at 460 nm disrupting both the Soret band and Q-band regions.

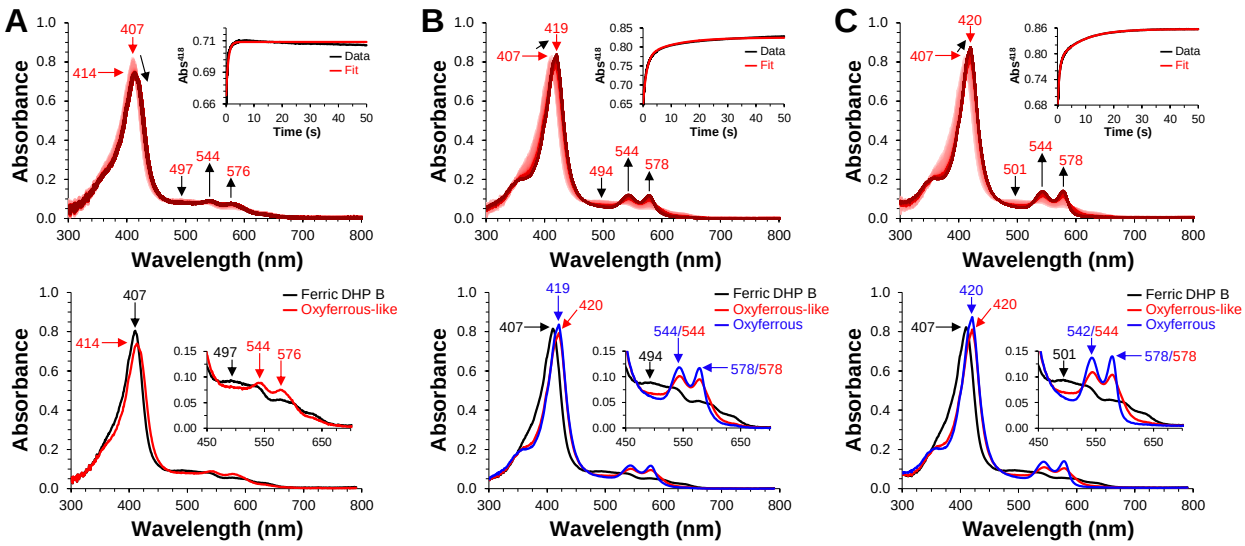


**Figure S9.** Stopped-flow spectroscopic monitoring of the reaction of ferric DHP B with 2-MeOBQ. **A) 0.625 µM 2-MeOBQ:** *top panel*, stopped-flow UV−visible spectra of the single-mixing reaction between ferric DHP B (8 µM) reacted with 0.625 µM 2-MeOBQ at pH 7.0 (900 scans over 50 s); inset: the single wavelength (418 nm) dependence on time obtained from the raw data (black) and fit (red); *bottom panel*, Calculated spectra of the two reaction components derived from the SVD analysis: Ferric DHP B (black) and oxyferrous-like DHP B (red). **B) 6.25 µM 2-MeOBQ:** *top panel*, stopped-flow UV−visible spectra of the single-mixing reaction between ferric DHP B (8 µM) reacted with 6.25 µM 2-MeOBQ at pH 7.0 (900 scans over 50 s); inset: the single wavelength (418 nm) dependence on time obtained from the raw data (black) and fit (red); *bottom panel*, Calculated spectra of the three reaction components derived from the SVD analysis: Ferric DHP B (black), oxyferrous-like DHP B (red), and oxyferrous DHP B (blue). **C) 625.0 µM 2-MeOBQ:** *top panel*, stopped-flow UV−visible spectra of the single-mixing reaction between ferric DHP B (8 µM) reacted with 625.0 µM 2-MeOBQ at pH 7.0 (900 scans over 50 s); inset: the single wavelength (418 nm) dependence on time obtained from the raw data (black) and fit (red); *bottom panel*, Calculated spectra of the three reaction components derived from the SVD analysis: Ferric DHP B (black), oxyferrous-like DHP B (red), and oxyferrous DHP B (blue).

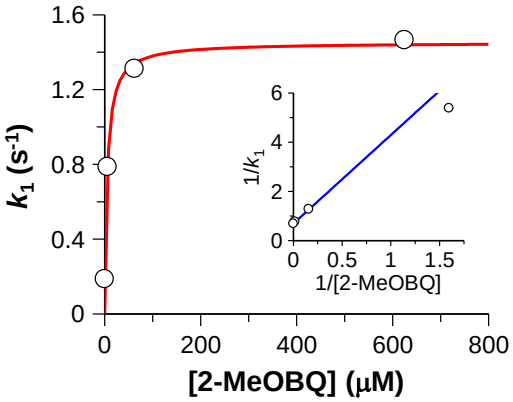


| [2-MeOBQ], μM | $k_1$ | $k_2$ |
|---|---|---|
| 0.625 | 0.186 (±0.006) | N/A |
| 6.25 | 0.786 (±0.005) | 0.093 (±0.003) |
| 62.5 | 1.311 (±0.004) | 0.227 (±0.001) |
| 625.0 | 1.465 (±0.004) | 0.117 (±0.001) |

N/A = not applicable, data fit to a single exponential

**Figure S10.** *Top*: plot of $k_{obs}$ vs [2-MeOBQ] using the data obtained from Figure S9 for the reduction of WT ferric DHP B by 2-MeOBQ (0.625-625 μM) yielding the oxyferrous-like DHP species; inset: corresponding double-reciprocal plot ($1/k_{obs}$ vs 1/[2-MeOBQ]). *Bottom*: rate constants determined from the SVD analysis data of the presented in Figure S9.